

Lipid concentrations in human coronary artery determined with high wavenumber Raman shifted light

Jonathan H. Nazemi

James F. Brennan III

Prescient Medical, Inc.

2005 South Easton Road, Suite 204

Doylestown, Pennsylvania, 18901

E-mail: jnazemi@prescientmedical.com

Abstract. Raman spectroscopy is a rapid nondestructive technique capable of assaying chemicals in human artery tissues and characterizing atherosclerotic plaques *in vivo*, but clinical applications through optical fiber-based catheters have been hindered by large background signals generated within the fibers. Previous workers realized that this background was reduced significantly in the high wavenumber (HWVN) Raman region ($\sim 2400\text{ cm}^{-1}$ to $\sim 3800\text{ cm}^{-1}$), and with proper selection of optical fibers, one could collect quality Raman spectra remotely via a single optical fiber with no additional filters or optics. This study compared lipid concentrations in coronary artery tissue that were determined with chemical assay techniques to those estimated from HWVN Raman spectra collected through a single optical fiber. The standard error of predictions between the Raman and chemical assay techniques were small for cholesterol and esterified cholesterols, at 1.2% and 2.7%, respectively. © 2009 Society of Photo-Optical Instrumentation Engineers. [DOI: 10.1117/1.3130302]

Keywords: Raman spectroscopy; atherosclerosis; vulnerable plaque; cardiovascular; fiber optic catheter.

Paper 09001RR received Jan. 7, 2009; revised manuscript received Mar. 16, 2009; accepted for publication Mar. 16, 2009; published online May 12, 2009.

1 Introduction

Among the diseases of the industrialized world, atherosclerosis is overwhelmingly the prime disorder that leads to serious morbidity and death. Although any artery may be affected, the aorta and the coronary and cerebral systems are the prime targets, with myocardial infarcts and strokes being two main consequences of the disease. The progression and regression of atherosclerotic plaques appear to be related to the amount and type of lipids that accumulate in the intima.^{1,2} The detection of these plaques that are vulnerable to rupture may be aided by classifying and quantifying the amounts of lipids, such as cholesterol and cholesterol esters, within the arterial wall.^{3,4}

Raman spectroscopy is a rapid nondestructive technique capable of assaying chemicals in human artery tissues and characterizing plaques *in vivo*.⁵⁻¹¹ However, clinical applications through optical fiber-based catheters have been hindered by large background signals generated within the fibers. Catheters that have been used *in vivo* commonly manage the fiber background by utilizing dedicated delivery and collection fibers equipped with filters and optics at the end of the fiber bundle, often leading to a catheter that is too bulky for routine cardiovascular use.¹²⁻¹⁴

Puppels and coworkers realized that the background signal generated from an optical fiber was reduced significantly in the high wavenumber (HWVN) Raman region ($\sim 2400\text{ cm}^{-1}$ to $\sim 3800\text{ cm}^{-1}$), and with proper selection of optical fibers, one could collect quality Raman spectra re-

motely via a single optical fiber with no additional filters or optics.¹⁵⁻¹⁷ These researchers pursued the technology and demonstrated that there were large differences between the HWVN Raman spectra of various structures and the components of the human coronary arterial wall.¹⁸

We have built upon this previous work by evaluating whether HWVN spectra can be used to quantify the relative concentrations of lipid components in the coronary artery. Although this study involved a limited sample population, the preliminary results are encouraging and warrant further investigation into this technique. We collected spectra of homogenized coronary artery tissue through a single optical fiber, developed a model of the spectra, and validated the model by comparing its estimated chemical concentrations to those measured by standard chemical assay techniques. The results verify that HWVN spectra measured through a single optical fiber can provide accurate compositional information of the human coronary artery and raise the possibility of determining this information *in vivo* via small-profile cardiovascular catheters.

2 Materials and Methods

The approach of this study was to compare lipid concentrations in coronary artery tissue that were estimated with HWVN spectra to lipid concentrations determined by chemical assay techniques. We used homogenized preparations of coronary artery tissue as opposed to ones with intact arterial walls, since the minimum volume of material needed for the chemical assays was much larger than that measured through

Address all correspondence to Jonathan Nazemi, Research and Development Prescient Medical, Inc., 2005 S. Easton Rd.—Suite 204, Doylestown, PA 18901; Fax: (267) 880-1900.

a single optical fiber (i.e. $<1 \text{ mm}^3$).^{8,19,20} This section describes the spectroscopic instrumentation, tissue preparation procedures, and analytical techniques.

2.1 Tissue Specimens

Human coronary arteries were acquired from the National Disease Research Interchange (NDRI, Philadelphia, PA). Arteries were dissected from the donor heart within 24 hours after death, snap-frozen in liquid nitrogen, and stored at -80°C until they were shipped on dry ice to our laboratory. They were stored at -20°C until their use several weeks later.

Coronary artery sections were prepared by thawing the tissue sections in phosphate buffered saline and then removing the adventitial layer from the coronary artery. The artery was opened longitudinally to expose the lumen surface, and the disease state was roughly assessed by gross examination. Isolated regions of interest, ranging from normal to advanced disease states, were submerged in liquid nitrogen and homogenized (BioPulverizer, BioSpec Products, Inc., Bartlesville, OK and SPEX 6770 Freezer/Mill, SPEX CertiPrep, Metuchen, NJ). Segments harvested from the same heart and exhibiting different stages of atherosclerosis were selectively combined before homogenization to produce tissue samples with varying amounts of specific lipid classes. Other methods of mechanically preparing samples were explored and found to be inferior. For example, preparations made by grinding the tissue in a ceramic mortar and pestle were contaminated with highly fluorescent particles.

The sample preparations were placed on a quartz microscope slide, compressed laterally between two 1-mm-thick quartz slides, and covered with a 100- μm -thick quartz coverslip. While the top slides were pushed together with the tissue between them, a slight downward pressure was applied on the coverslip until the tissue was well distributed throughout the resulting cavity and in good contact with the coverslip. The tissue within the cavity was 1 mm deep, with a width and length determined by the volume of the specific sample.

2.2 Raman Spectra Acquisition and Processing

Raman spectra in the HWVN shifted region (2200 cm^{-1} to 3600 cm^{-1}) were collected with a River Diagnostics HPRM2500 (Rotterdam, The Netherlands), that had been modified from its original free-space configuration to accept a single-fiber input. The system included a custom reflective-grating spectrometer, a CCD camera (iDus CCD40-11, Andor, Belfast, Ireland), and a 671-nm diode-pumped solid state laser (CrystaLaser, Reno, NV). The system was measured to have a spectral resolution of $\sim 5 \text{ cm}^{-1}$ by determining the FWHM of the 2852.9 cm^{-1} Raman feature of cyclohexane. The instrument was calibrated for wavenumber shift by interpolating between six known locations of spectral features of cyclohexane (2664.4 cm^{-1} , 2852.9 cm^{-1} , and 2938.3 cm^{-1}) and acetaminophen (2931.1 cm^{-1} , 3064.5 cm^{-1} , and 3102.4 cm^{-1}).

Excitation light was directed down a single 105- μm -core 0.22-NA silica optical fiber that was 3 m in length.¹⁷ The resulting scattered light from the sample was collected by the same fiber and directed into the spectrometer. The distal end of the fiber was epoxied (H05-100-R2, Fiber Instrument Sales, Oriskany, NY) into a stainless steel hypotube and pol-

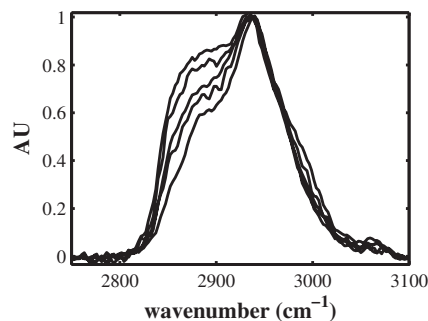


Fig. 1 Spectra representing the variation within the calibration data.

ished flat. The typical laser power exiting the fiber was $\sim 75 \text{ mW}$. The spectral response of the system was calibrated by placing the fiber probe against a poly(tetrafluoroethylene) block and irradiating the sample with a tungsten-halogen light source (LS-1, Ocean Optics, Dunedin, FL).

The sample holder was placed onto a translation stage, and the fiber probe was placed $\sim 100 \mu\text{m}$ from the surface of the coverslip. Spectra were taken from hundreds of locations throughout the sample volume with 500-ms measurement durations at each location. All the spectra collected from a given sample were combined to produce a single average spectrum.

Background signals were removed from the spectra by fitting a third-order polynomial to the regions outside the Raman signature and then subtracting the fitted polynomial. The remainder was normalized by fitting a second-order polynomial in the 2932 cm^{-1} to 2942 cm^{-1} region and dividing it by the maximum value in the polynomial fit, producing a normalized HWVN spectrum.

2.3 Chemical Assays

Each sample was sent to the Lipoprotein Analytic Laboratory at the Wake Forest Medical Center (Wake Forest University School of Medicine, Department of Pathology, Wake Forest, NC) to undergo a series of chemical assays that would determine the absolute weight of free (nonesterified) cholesterol (FC), cholesterol esters (CE), phospholipids (PL), triglycerides (TG), and proteins (PT). These results were then converted into relative concentrations by dividing the weight of each component by the sum of the weights of all five components. The lipid assay was described by Carr, Andresen, and Rudel;²¹ the protein assay was conducted with the modified Lowry assay.²²

We assessed the reproducibility of the chemical assays by dividing one large homogenized tissue sample into nine portions and then submitting each portion separately for analysis. The standard deviation between the relative concentrations for each compound was found to be: FC, $\sim 0.1\%$; CE, $\sim 0.3\%$; PL, $\sim 0.1\%$; TG, $\sim 0.4\%$; and PT, $\sim 0.8\%$.

3 Model Development

A model of the HWVN spectra was developed with a calibration data set consisting of spectra and assay values from 14 unique homogenized tissue samples. Example spectra from the calibration set spectra are shown in Fig. 1, which demonstrates how the spectral features varied among samples in the data set. The chemical assay results ranged for FC from $\sim 0\%$

Table 1 Correlation coefficients R^2 between assay results for each chemical compound in the calibration data set.

	FC	CE	TG	PL	PT
FC	1.0	0.66	0.24	0.45	0.52
CE	—	1.0	0.14	0.24	0.61
TG	—	—	1.0	0.16	0.03
PL	—	—	—	1.0	0.23
PT	—	—	—	—	1.0

to $\sim 22\%$; CE, $\sim 4\%$ to $\sim 29\%$; TG, $\sim 0\%$ to $\sim 30\%$; PL, $\sim 1\%$ to $\sim 8\%$; and PT, $\sim 40\%$ to $\sim 90\%$. A matrix of the squared correlation coefficients R^2 , which was used to check for the independence of the chemical components, is given in Table 1. The spectra in the calibration set were decomposed with principle component analysis (PCA), and the first four dominant factors were retained, since the minimum standard error of calibration (SEC) occurred at that point for all components.^{23,24}

Prediction vectors for FC, CE, TG, PL, and PT, which are shown in Fig. 2, were calculated with the four factors and the assay results. The prediction vectors provided an estimate for a given chemical concentration when a spectrum was projected onto them. An initial assessment of the predictive ability of this model was made by retrospectively examining the calibration data set. The SEC for FC was 3.0%; CE, 3.3%; TG, 2.1%; PL, 1.4%; and PT, 5.0%. Charts comparing these model estimates with the chemical assay results are shown in Fig. 3. The hundreds of spectra taken from each sample were individually processed to assess the residual inhomogeneity in a given tissue preparation; the error bars in Fig. 3 indicate the standard deviation of the calculated values.

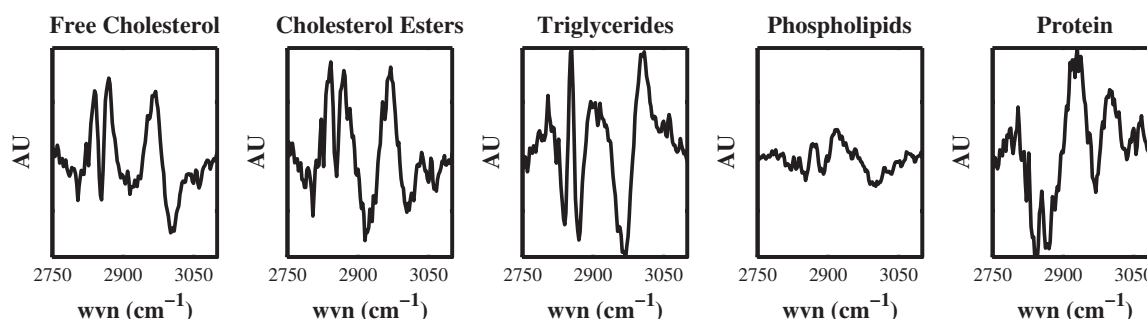
Other techniques for processing the spectra were performed, such as partial least squares and classical least squares, but were found to be more susceptible to errors with decreasing signal-to-noise ratios of the spectra.^{23,24} All numerical analyses were performed using Matlab® loaded with the Statistics Toolbox (The MathWorks, Inc., Natick, MA).²⁵

4 Model Validation

We created a validation data set ($N=7$) to assess the predictive ability of the HWVN spectra model. Tissue preparation and data collection were performed with the same protocol used for the calibration set. The relative component concentrations determined by chemical assay for the validation set ranged for FC from $\sim 0\%$ to $\sim 6\%$; CE, $\sim 1\%$ to $\sim 14\%$; TG, $\sim 2\%$ to $\sim 22\%$; PL, $\sim 1\%$ to $\sim 7\%$; and PT, $\sim 75\%$ to $\sim 87\%$.

The spectra were processed and analyzed with the model to estimate chemical concentrations. Numerical comparisons between the model predictions and the chemical assay results are listed in Table 2, which details for each component the standard error of prediction (SEP) and linear regression analysis slopes (m), y-axis intercepts (y_0), squared correlation coefficients (R^2), and P-values.^{23,24} Graphical representations of the regression results are in Fig. 4 (left-side plot for each component), where the error bars indicate the standard deviation of the values calculated from all individual spectra taken from a given sample.

We utilized Bland-Altman analysis²⁶ to compare the differences between the chemical assay and model estimates as shown in Fig. 4, (right-side plot for each component). The means ($\bar{\Delta}$) and standard deviations (s) of the comparison differences are also listed in Table 2 along with the 95% confidence intervals for each parameter.

**Fig. 2** Prediction vectors calculated using the four primary PCA vectors and chemical assay results.

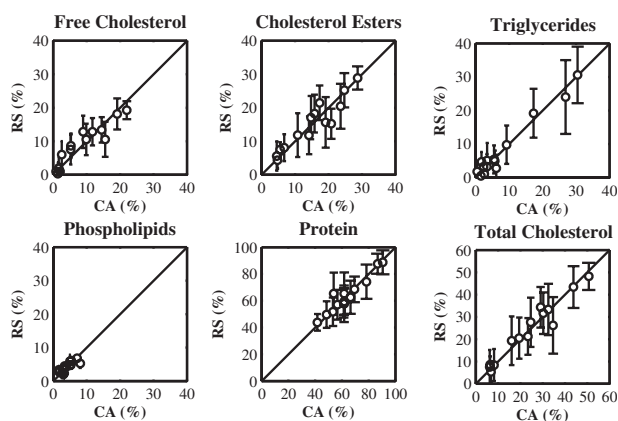


Fig. 3 Retrospective comparison between the chemical assay (CA) results and the estimates made with the Raman spectra (RS) for each chemical component in the calibration data. The diagonal line is the 1:1 correlation line.

The comparison data for all the cholesterols, FC and CE, were combined to form a total cholesterol (TC=FC+CE) category, which was also examined for prediction accuracy with numerical values listed in Table 2 and a graphical comparison given in Fig. 4.

5 Discussion

The Bland-Altman analysis of the validation data set shows that HWVN Raman spectra analysis can quantify the relative weights of cholesterols that are present in coronary artery tissue to within a maximum error of a few percentage points. These results were obtained over a range where TC was ~20% or less; a larger data set that covers a broader range may have a different outcome. The mean difference between the Raman and chemical assay techniques for the total cholesterol content TC was ~3.3%. For FC and CE, the differences were <1% and ~2.6%, respectively, with corresponding regression correlations of high statistical significance. Although the mean difference in PL was also very small at ~0.5%, a poor correlation was calculated between the two assay techniques. This was likely due to the narrow content

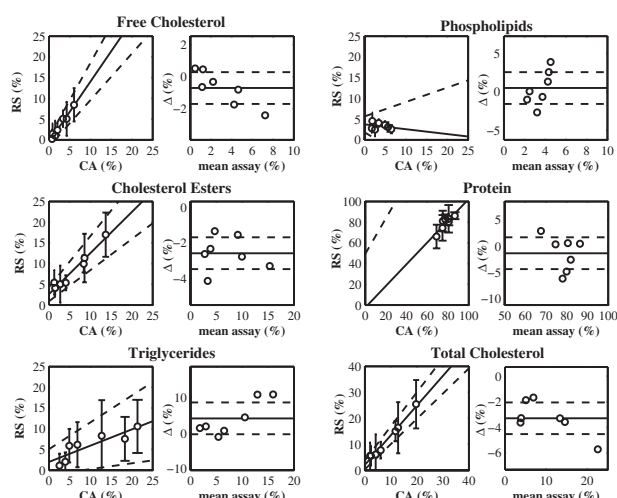


Fig. 4 Comparison between the chemical assay (CA) results and the estimates made with Raman spectra (RS) for each chemical component and the total cholesterol in the validation data. For each component, a linear regression with the comparison data set is plotted on the left side (solid line), while the right side displays the Bland-Altman analysis of the mean ($\bar{\Delta}$) difference between the measurements (solid lines). The dashed lines indicate 95% confidence intervals.

range of PL in the validation set, making PL estimates unreliable. The estimates of TG content compared to the assay results were too low, as indicated by the strongly correlated regression slope of 0.4 and a mean difference of $4.6 \pm 4.5\%$. However, PT was accurately estimated with a ~1.3% mean error, a strong correlation, and a ~1.0 regression slope. The 95% confidence intervals of the PT linear regression parameters were large, which was likely due to the limited range covered by the data set. Strong trends are not apparent in the Bland-Altman graphs, although FC appears to be underestimated and TG overestimated with increasing concentration levels. These results are similar to those obtained in earlier work in the Raman fingerprint region.⁸ The salient addition of this current study is that these estimates of compound concentrations were made with spectra gathered through a single optical fiber.

Table 2 Comparison data between the standard assay and spectra model estimates with the validation data set.

Comp.	SEP (%)	Regression Analysis				Bland-Altman Analysis	
		m	y_0	R ²	P	$\bar{\Delta}$ (%)	s (%)
FC	1.2	1.5±0.3	-0.5±1.1	0.96	<0.001	-0.7±1.0	1.1±0.4
CE	2.7	1.0±0.2	2.6±1.7	0.96	<0.001	-2.6±0.9	1.0±0.3
TG	6.1	0.4±0.3	2.0±3.1	0.76	<0.05	4.1±4.5	4.8±1.7
PL	2.1	-0.1±0.5	3.7±2.0	0.08	0.55	0.5±2.1	2.2±0.8
PT	3.3	1.0±0.6	-2.5±51.9	0.77	<0.01	-1.3±3.0	3.3±1.2
TC	3.0	1.1±0.2	2.1±1.8	0.98	<0.001	-3.3±1.2	1.3±0.5

Our technique for analyzing the HWVN Raman spectra was developed to quantify the content of specific lipids in the arterial wall. Other compounds, such as specific proteins, glycosaminoglycans, and DNA, are also present in arteries, and it may be possible to expand the current spectral model to quantify the concentrations of these compounds. In future work, it also may be possible to quantify macromolecules, such as lipoproteins, and identify more lipids, such as specific phospholipids and cholesterol esters.

6 Study Limitations

Correlations exist in the calibration data between FC and CE, as well as between each cholesterol category and protein, which may have reduced the number of independent variables in the model development. Although these correlations are as expected when examining atherosclerotic tissue,^{3,4} they may have limited the number of PCA factors in our study. A larger calibration data set may be needed, perhaps with added lipid extracts, to weaken internal correlations within the data set and refine the existing model.

Homogenized coronary arteries were used in this study because previous studies on intact (unground) coronary artery sections gave considerable spread to the Raman assay data as measured against chemical assays.²⁷ We concluded that point-to-point spatial variations in the structure of arterial lesions made it difficult to compare the small region examined with Raman spectroscopy with the much larger volume examined by conventional assay. Compounds that are present in large concentrations near the luminal surface of the artery but not significantly present at locations deeper than the artery intima will be diminished in concentration via the homogenization process and may become undetectable. Our ongoing studies compare HWVN Raman spectra with an intact arterial wall. Studies are also underway to assess the performance of this technology with spectra collected by sideways-looking probes in a blood field using cadaver arteries grafted onto living porcine hearts.²⁸ Initial results indicate that measurement durations of a few hundred milliseconds can provide spectra of sufficient quality for accurate composition estimates, but more work needs to be done to assess the effects of blood and collection times on the model estimates.

7 Conclusions

In this exploratory study, we have demonstrated that the relative chemical composition of a coronary artery can be determined with HWVN Raman spectra collected through a single optical fiber, allowing the possibility of small-profile catheters for routine cardiovascular applications. The algorithms presented here are being integrated into a catheter-based system that can collect quality HWVN spectra from coronary arteries, allowing characterization of the coronary artery wall *in vivo*, and may act as a diagnostic tool for the detection of vulnerable plaques. Although this study involved a limited sample population, these preliminary results are encouraging and warrant further investigation into this technique.

Acknowledgments

We would like to thank Martha Wilson, PhD, from the department of pathology at the Wake Forest University School of

Medicine for performing the biochemical assays for this study. We would also like to thank Prescient Medical, Inc. for allowing this material to be released.

References

1. R. S. Cotran, V. Kumar, and S. L. Robbins, "Blood Vessels," Chap. 12 in *Robbins Pathologic Basis of Disease*, 4th ed., W. B. Saunders Company, Philadelphia, PA (1989).
2. D. P. Zipes, P. Libby, R. O. Bonow, and E. Braunwald, *Braunwald's Heart Disease*, 7th ed., Elsevier Saunders, Philadelphia, PA (2005).
3. R. Virmani, J. Narula, M. B. Leon, and J. T. Willerson, *The Vulnerable Atherosclerotic Plaque: Strategies for Diagnosis and Management*, Blackwell Publishing, Malden, MA (2007).
4. C. V. Felton, D. Crook, M. J. Davies, and M. F. Oliver, "Relation of plaque lipid composition and morphology to the stability of human aortic plaques," *Arterioscler., Thromb., Vasc. Biol.* **17**, 1337–1345 (1997).
5. R. Manoharan, J. J. Baraga, M. S. Feld, and R. P. Rava, "Quantitative histochemical analysis of human artery using Raman spectroscopy," *J. Photochem. Photobiol., B* **16**(2), 211–33 (1992).
6. J. J. Baraga, M. S. Feld, and R. P. Rava, "Rapid near-infrared Raman spectroscopy of human tissue with a spectrograph and a CCD detector," *Appl. Spectrosc.* **46**, 187–190 (1992).
7. J. J. Baraga, M. S. Feld, and R. P. Rava, "In situ optical histochemistry of human artery using near infrared Fourier transform Raman spectroscopy," *Proc. Natl. Acad. Sci. U.S.A.* **89**(8), 3473–3477 (1992).
8. J. F. Brennan, T. J. Romer, R. S. Lees, A. M. Tercyak, J. R. Kramer, and M. S. Feld, "Determination of human coronary artery composition by Raman spectroscopy," *Circulation* **96**, 99–105 (1997).
9. T. J. Romer, J. F. Brennan, M. Fitzmaurice, M. L. Feldstein, G. Deinum, J. L. Myles, J. R. Kramer, R. S. Lees, and M. S. Feld, "Histopathology of human coronary atherosclerosis by quantifying its chemical composition with Raman spectroscopy," *Circulation* **97**, 878–885 (1998).
10. L. Silveira, S. Sathaiyah, R. A. Zangaro, M. T. T. Pacheco, M. C. Chavantes, and C. A. G. Pasqualucci, "Correlation between near-infrared Raman spectroscopy and the histopathological analysis of atherosclerosis in human coronary arteries," *Lasers Surg. Med.* **30**, 290–297 (2002).
11. J. T. Motz, M. Fitzmaurice, A. Miller, S. J. Gandhi, A. S. Haka, L. H. Galindo, R. R. Dasari, J. R. Kramer, and M. S. Feld, "In vivo Raman spectral pathology of human atherosclerosis and vulnerable plaque," *J. Biomed. Opt.* **11**, 021003–021009 (2006).
12. H. P. Buschman, E. T. Marple, M. L. Wach, B. Bennett, T. C. Bakker-Schut, H. A. Bruining, A. V. Brusckhe, A. v. d. Laarse, and G. J. Puppels, "In vivo determination of the molecular composition of artery wall by intravascular Raman spectroscopy," *Anal. Chem.* **72**, 3771–3775 (2000).
13. U. Utzinger and R. R. Richards-Kortum, "Fiber optic probes for biomedical optical spectroscopy," *J. Biomed. Opt.* **8**(1), 121–147 (2003).
14. J. T. Motz, M. Hunter, L. H. Galindo, J. A. Gardecki, J. R. Kramer, R. R. Dasari, and M. S. Feld, "Optical fiber probe for biomedical Raman spectroscopy," *Appl. Opt.* **43**(3), 542–554 (2004).
15. S. Koljenović, T. C. Bakker-Schut, R. Wolthuis, B. de Jong, L. Santos, P. J. Caspers, J. M. Kros, and G. J. Puppels, "Tissue characterization using high wave number Raman spectroscopy," *J. Biomed. Opt.* **10**(3), 031116 (2005).
16. S. Koljenović, T. C. Bakker-Schut, R. Wolthuis, A. Vincent, G. Hendriks-Hagevi, L. F. Santos, J. Kros and G. J. Puppels, "Raman spectroscopic characterization of porcine brain tissue using a single fiber-optic probe," *Anal. Chem.* **79**(2), 557–564 (2007).
17. L. F. Santos, R. Wolthuis, S. Koljenović, R. M. Almeida, and G. J. Puppels, "Fiber-optic probes for *in vivo* Raman spectroscopy in the high-wavenumber region," *Anal. Chem.* **77**, 6747–6752 (2005).
18. S. W. E. van de Poll, "Raman spectroscopy of atherosclerosis," PhD thesis, University of Leiden, The Netherlands, (2003).
19. T. J. Römer, J. F. Brennan, T. C. Bakker-Schut, R. Wolthuis, R. C. M. van den Hoogen, J. J. Jemeis, A. van der Laarse, A. V. G. Brusckhe, and G. J. Puppels, "Raman spectroscopy for quantifying cholesterol in intact coronary artery wall," *Atherosclerosis* **141**(1), 117–124 (1998).
20. A. Chau and G. Tearney, "Preliminary report on Monte Carlo sampling volume modeling," Wellman Center for Photomedicine, Cam-

- bridge, MA (2007).
21. T. P. Carr, C. J. Andresen, and L. L. Rudel, "Enzymatic determination of triglyceride, free cholesterol, and total cholesterol in tissue lipid extracts," *Clin. Biochem.* **26**, 39–42 (1993).
 22. O. H. Lowry, N. J. Rosebrough, A. L. Farr, and R. J. Randall, "Protein measurement with the folin phenol reagent," *J. Biol. Chem.* **193**, 265–275 (1951).
 23. K. R. Beebe, R. J. Pell, and M. B. Seasholtz, *Chemometrics: A Practical Guide*, Wiley, New York (1998).
 24. R. Kramer, *Chemometric Techniques for Quantitative Analysis*, CRC Press, Boca Raton, FL (1998).
 25. The MathWorks, Inc., Matlab Version # 7.6.0.324, Statistics Toolbox Version #6.2 Natick, MA, www.mathworks.com.
 26. J. M. Bland and D. G. Altman, "Statistical methods for assessing agreement between two methods of clinical measurement," *Lancet* **8**, 307–310 (1986).
 27. J. F. Brennan, "Near infrared Raman spectroscopy for human artery histochemistry and histopathology," PhD thesis Massachusetts Institute of Technology, Cambridge, MA, (1995).
 28. J. F. Brennan, J. Nazemi, J. Motz, and S. Ramcharitar, "The vPredict™ optical catheter system: Intravascular Raman spectroscopy," *EuroIntervention* **3**, 635–638 (2008).